Hybrid silica-organic material with immobilized amino groups: surface probing and use for electrochemical determination of nitrite ions

Oleg Tkachenko, Abdur Rahim, Andrey Baraban, Ruslan Sukhov, Inna Khristenko, Yoshitaka Gushikem & Yuriy Kholin

Journal of Sol-Gel Science and Technology

ISSN 0928-0707

J Sol-Gel Sci Technol
DOI 10.1007/s10971-013-3060-3

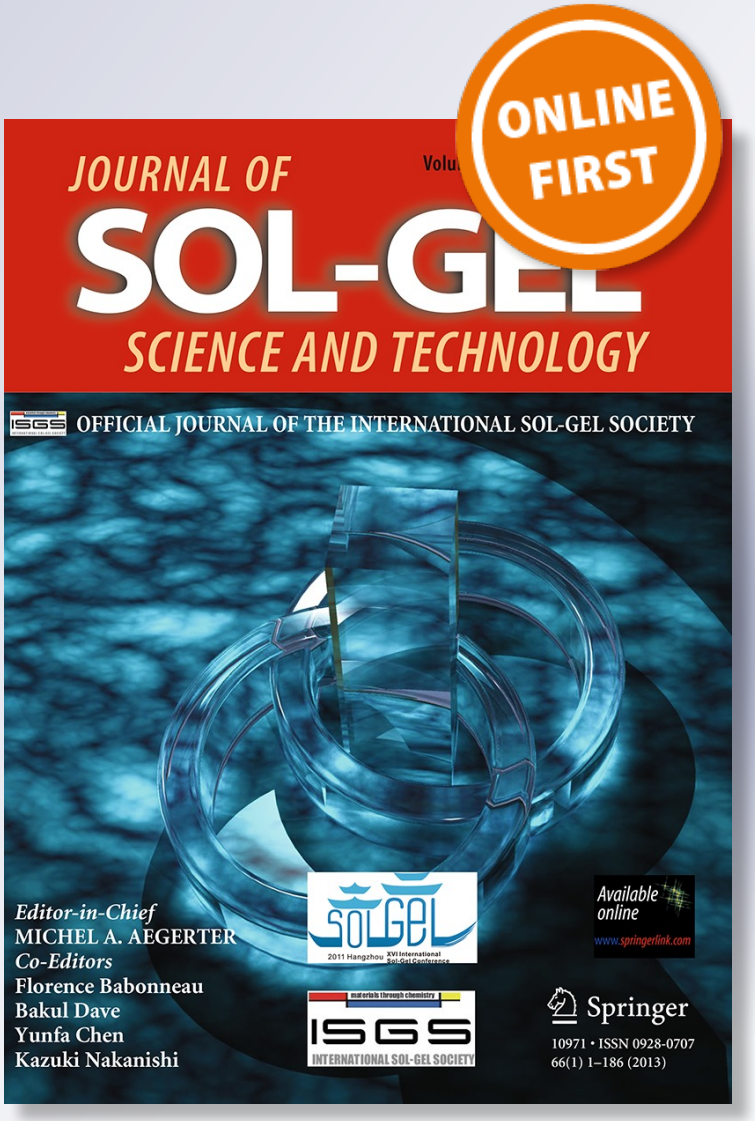

Springer

J Sol-Gel Sci Technol
DOI 10.1007/s10971-013-3060-3

ORIGINAL PAPER

Hybrid silica-organic material with immobilized amino groups: surface probing and use for electrochemical determination of nitrite ions

Oleg Tkachenko · Abdur Rahim · Andrey Baraban · Ruslan Sukhov · Inna Khristenko · Yoshitaka Gushikem · Yuriy Kholin

Received: 10 January 2013 / Accepted: 29 April 2013

Abstract Hybrid silica-organic material with fixed *n*-propylamine groups was prepared by a sol–gel route and characterized by several techniques. Specific surface area of the material was 110 ± 2 m^2 g^{-1}, specific pore volume was 0.90 ± 0.01 cm^3 g^{-1}, and average pore size was 25 ± 3 nm. The specific concentration of attached amino groups was 3.28 ± 0.05 mmol g^{-1}, the amount of residual silanol groups being comparable with that of amino groups. The maximum attainable adsorption of H^+ ions was 2.34 ± 0.10 mmol g^{-1}. The Dimroth–Reichardt normalized polarity parameter of the near-surface layer was 0.64 that points to the closeness of properties of the near-surface layer to those of water-organic mixtures and polar organic solvents rather than aqueous solutions. Surface probing with H^+ ions has revealed that due to interactions between surface amino groups and weakly acidic silanol groups the protonization constants of fixed amino groups are considerably smaller than the protonization constants of aliphatic amines in aqueous solutions. The equimolecular composition of Cu (II) complexes with immobilized amino groups was concluded from the results of surface probing with Cu^{2+} ions and UV–vis diffuse reflectance spectroscopy. The stability constants of Cu (II) complexes were determined with the aid of the model of polydentate binding, and the influence of strong negative cooperativity effects on the adsorption equilibria was detected. The material with sorbed Cu (II) ions was used to prepare a working electrode for the electrochemical determination of nitrite ions. The electrocatalytic determination of nitrite ions in aqueous media may be performed by means of cyclic voltammetry, differential pulse voltammetry and chronoamperometry with the limits of detection 1.3, 4.6, and 3.1 μmol l^{-1}, correspondingly.

Keywords Hybrid silica-organic material · Probing · Nitrite · Electrochemical determination

1 Introduction

At present, hybrid silica-organic materials are extensively developed and studied [1, 2]. The sol–gel method is the most convenient way to obtain materials with the controlled morphology and physicochemical properties. Hybrid materials containing organic moieties are often used in adsorption, catalysis, preparation of optical and electrochemical sensors [3–7]. In particular, some materials prepared by the sol–gel method (for instance, silica–cerium mixed oxides [8], SiO_2/SnO_2 carbon ceramic composite [9], SiO_2/SnO_2 network mixed with 3-n-propylpyridinium chloride silsesquioxane with sorbed cobalt(II) tetrasulfonate [7]) were used for the electrochemical determination of nitrite ions. Nitrite ions have high carcinogenic, teratogenic and toxic effects. Their concentration is an important water pollution index. Maximum admissible concentration of nitrite in drinking water is established at levels varied from 0.5 to 3.0 mg l^{-1} [10, 11]. So, the control of the content of nitrite ions is considered as an important element of the environmental monitoring. As the concentration of nitrite ions in natural objects is low, and many coexistent substances can affect their

O. Tkachenko · A. Baraban · R. Sukhov · I. Khristenko · Y. Kholin (✉)
V.N. Karazin Kharkiv National University, 4 Svoboda Square, Kharkiv 61022, Ukraine
e-mail: kholin@univer.kharkov.ua

O. Tkachenko · A. Rahim · Y. Gushikem
Institute of Chemistry, State University of Campinas, PO Box 6154, Campinas, SP 13083-970, Brazil

Published online: 08 May 2013

determination, the analytical procedures should be simple, rapid, sensitive and accurate. Nitrite ions are usually determined by spectrophotometric [12], chromatographic [13, 14] and, more recently, by electrochemical methods [15, 16]. The electrochemical determination of nitrite is based on its reduction or oxidation. Methods based on the reduction usually suffer from poor sensitivity and are subjected to several interferences [17, 18]. The electrochemical oxidation is a direct reaction leading to nitrate ion [19]. Nitrite ions behave as electroactive species when exposed to different electrodes that stimulate the development of new electrochemical sensors for their determination.

In this work new hybrid silica-organic material with fixed groups of *n*-propylamine prepared by the sol–gel method was characterized and after sorption of Cu (II) ions used for the determination of nitrite ions by cyclic voltammetry (CV), differential pulse voltammetry (DPV) and chronoamperometry (ChA). To the best of our knowledge, till now such materials were not applied for solving this task. It is noteworthy that amperometric sensor for dissolved oxygen was successfully developed on the base of Cu (II) complex with 3-aminopropyltriethoxysilane immobilized on silica gel [20]. This suggests that similar objects can be used in the creation of electrochemical sensors for another oxidizable species.

2 Experimental

2.1 Reagents and solutions

The following reagents were used: tetraethoxysilane (TEOS) and 3-aminopropyltriethoxysilane (APTES) (both Merck, 98 %), graphite (99.99 %) and standard Reichardts' solvatochromic betaine dye 2,6-diphenyl-4-(2,4,6-triphenylpyridinium-1-yl)phenolate (ET(30), ≥95 % dye) (both Aldrich), HNO_3 (Nuclear, 70 %), HCl (99 %), $CuSO_4 \cdot 5H_2O$ (98 %) and KNO_3 (99 %, all three Reachim, Russia), ethanol (Dubov'yazivka Distillery, Ukraine, 96 %), $NaNO_2$ and KCl (both Synth, Sao Paulo, Brazil, 99 %). Reichardts' betaine dye 2,6-dichloro-4-(2,4,6-triphenyl-N-pyridino)-phenolate (ET(33), ≥95 % dye) was synthesized and purified as described elsewhere [21, 22]. The standard buffer solutions with pH 1.68, 3.56, 4.01 and 6.86, 9.18 were purchased from Reachim, Russia. The Britton–Robinson buffer solutions were prepared as described elsewhere [23].

All aqueous solutions were prepared using doubly distilled and deionized water with the resistivity not higher than 18.2 MW cm at 293 K. Stock $CuSO_4$ ($\sim$0.1 mol l^{-1}) and $NaNO_2$ (0.05 mol l^{-1}) solutions were prepared by direct dissolution of salts in water. The concentration of the stock $CuSO_4$ solution was determined by the chelatometry titration with the Trilon B 0.052 mol l^{-1} solution in the presence of murexide as indicator. The work solutions were obtained by the dilution. The solutions of ET(30) and ET(33) were prepared by the dissolution of exact weights of the dyes in 20.0 ml of ethanol.

Before voltammetry or amperometry experiments, the dissolved oxygen was removed from solutions by bubbling high purity nitrogen.

2.2 Synthesis of hybrid silica-organic material

The hybrid silica-organic material under study was prepared according to the slightly modified procedure [24]: 20 ml of ethanol were added to the mixture of 2.4 ml APTES and 5.6 ml TEOS, stirred for 5 min, and then 8 ml of distilled water were added. The obtained gel was vigorously stirred for 35 min. The mixture was kept at 293 K for 24 h. After that the obtained gel was filtered and dried in the microwave oven at 70 W for 15 min and then at 150 W for 10 min.

2.3 Characterization

The morphology of the material was characterized by means of transmission electron microscopy with the use of a TEM-125 K microscope (Selmi, Ukraine). The C, H, N elemental analysis was executed on a 2400 CHN Elemental Analyzer apparatus (Perkin Elmer). N_2 adsorption–desorption isotherms were measured at 77 K on a Nova Station B apparatus (Quantachrome Instruments). The samples were previously outgassed at 353 K for 4 h. The Brunauer-Emmett-Teller method [25] was employed to calculate the specific surface area (S_{BET}). Solid-state nuclear magnetic resonance spectroscopy for ^{13}C and ^{29}Si (CP/MAS NMR) was performed on a AC300/P spectrometer (Bruker) operating at 100.6 MHz for ^{13}C (pulse sequences with 4 ms contact time, an interval between pulses of 1 s and an acquisition time of 0.041 s) and at 79.5 MHz for ^{29}Si (pulse sequences with 3 ms contact time, an interval between pulses of 2 s and acquisition time of 0.041 s). Adamantane and kaolinite were used as external references for the ^{13}C and ^{29}Si chemical shifts, correspondingly. The thermogravimetric analysis was performed with the use of a TGA 2050 apparatus (TA Instruments). The sample was heated from 30 to 700 °C (10 °C min^{-1}) under the oxygen atmosphere.

To measure pH and pCu of solutions, the galvanic circuits with glass electrode with hydrogen function ES-10603 (for pH) or copper ion-selective electrode ELIS-131Cu (for pCu), reference Ag/AgCl electrode EVL-1M3 (all electrodes from KhimLaborReactive, Ukraine) and salt bridge filled with saturated KNO_3 solution in agar were

used. The electromotive forces were measured with the laboratory ion meter U-160 Mu (Izmeritelnaya Tekhnika IT, Russia). The galvanic circuits were calibrated with the standard pH buffer solutions (for pH measurement) and 5×10^{-5}–1×10^{-1} mol l^{-1} $CuSO_4$ solutions in 0.1 mol l^{-1} KNO_3 solution (for pCu). All measurement were performed at 293 ± 2 K. The errors of measurements did not exceed 0.03 for pH and 0.04 for pCu, and the suspension effect did not exceed 0.1 pH or pCu in all cases.

Preliminary experiments have shown that time necessary for suspensions of the material to achieve a stationary state after addition of HCl solution do not exceed 1 h (at pH values in the equilibrium state from 2 to 7.5). For this reason the procedure of the pH-metric titration of one sample was used to probe the material surface with H^+ ions. 20.0 ml of water were added to precise weights (~0.1 g) of the material, and the obtained suspensions were titrated with the 0.1 mol l^{-1} HCl solution. The ionic strength of solutions (0.1 mol l^{-1}) was maintained with KNO_3.

To probe the material with Cu (II) ions, the batch technique was applied. Precise weights of the material (~0.1 g) were suspended in 15.0–20.0 ml of distilled water, and 1–10 ml of $CuSO_4$ solutions (0.001–0.1 mol l^{-1}) were added to the suspensions. The pH values of solutions (3–7) were retained by the addition of 0.1 mol l^{-1} HCl solution. The mixtures were stirred and stored for 24 h in the closed weighing bottles. Then pH and pCu were measured. Specific concentrations of the adsorbed H^+ or Cu^{2+} ions were calculated as

$$N_f = \frac{N_i - [\mathrm{M}] \cdot V}{m_s} \quad (1)$$

where M is H^+ or Cu^{2+}; N_i is the initial amount of M in solution (mol); V is the volume of aqueous phase (l), and m_s is the mass of the material (g).

Ultraviolet/visible (UV–vis) diffuse reflectance spectra of the material with sorbed Cu^{2+} ions or deposited ET(33) were recorded on an UV–vis-NIR-5000 spectrophotometer (Agilent Technologies) with $BaSO_4$ as the standard of reflection. The values of the Kubelka–Munk function were calculated from the measured reflections ($0 < R < 1$) as

$$F = \frac{(1-R)^2}{2R}. \quad (2)$$

Solvatochromic dyes ET(30) and ET(33) were deposited onto the material sample (0.3 g) from 3.0 ml of the dye solutions of certain concentrations in ethanol. The suspensions were stirred for 20 min and then left to stand for 24 h at a room temperature (~293 K) in the open weighing bottles. Ethanol was removed by the evaporation at ~100 °C for 1 h. Ethanol was selected as a solvent because it does not interact with surface groups under experimental conditions, is more basic than a probe, and is volatile. The samples with deposited dyes were kept at a room temperature in a vacuum desiccator over concentrated sulphuric acid. Also, part of the samples was stored in air conditions.

Large amounts of the material with different amounts of sorbed Cu (II) were obtained according to the following procedure: exact weights of the material (~0.5 g) were suspended in 20.0 ml of $CuSO_4$ solutions with different concentrations (Table 1). 0.1 Mol l^{-1} HCl solution was used to maintain pH = 5.8 ± 0.2. The mixtures were stirred for 5 min in closed flasks and then kept for 48 h at a room temperature. After that the solids were separated by filtration, and the residual Cu (II) concentrations in solutions were determined by the ionometric method.

2.4 Simulation of adsorption equilibria

The model of polydentate binding [3] was used to simulate the H^+ and Cu^{2+} adsorption equilibria. This model considers the surface as an assemblage of polydentate centers $\overline{Q_Z}$, each center being constituted from Z active groups Q. The specific concentration of centers $\overline{Q_Z}$ is t_Q/Z, where t_Q is the specific concentration of active groups (mol g^{-1}). The binding of a sorbate species by centers $\overline{Q_Z}$ is treated as the stepwise process. The binding equilibrium is described by Z values of equilibrium constants $\beta_i^{(Z)}$, where i is the step number. Figure 1 illustrates the description of the H^+ adsorption by a variant of this model.

The fitting parameters (size of a polydentate center Z and equilibrium constants $\beta_i^{(Z)}$, $i = 1, 2, \ldots, Z$) were determined through the approximation of the composition-property dependences by the model [3]. The quality of approximation was estimated by the value of criterion

$$\chi^2_{\mathrm{exp}} = \sum_{k=1}^{N} \xi_\kappa^2 \quad (3)$$

where k is the number of the experimental points, N is the total number of points, weighed discrepancy $\xi_\mathrm{k} = w_\mathrm{k}^{1/2} \cdot \Delta_\mathrm{k}$, discrepancy $\Delta_\mathrm{k} = \mathrm{A}_\mathrm{k}^{\mathrm{theoretical}} - \mathrm{A}_\mathrm{k}^{\mathrm{experimental}}$, A is the value of the measured property of the equilibrium system (N_f, $[H^+]$, or $[Cu^{2+}]$), w_k, the statistical weights of measurements, were assigned as $w_k = \frac{1}{A_k^2 \sigma_r^2}$, where σ_r is the

Table 1 Data on samples with sorbed Cu (II) ions

Samples	m_s/g	$c(CuSO_4)$/ mol l^{-1}	N_f/ mmol g^{-1}	λ_{max}/ nm	F
A	0.5280	0.02	0.75	720	0.14
B	0.5045	0.04	1.24	730	0.23
C	0.5180	0.09	1.68	735	0.31

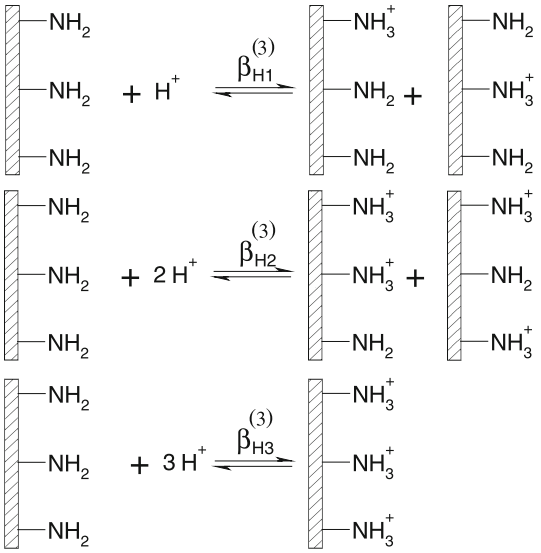

Fig. 1 Representation of the H^+ interaction with immobilized amino groups by the model of tridentate binding ($Z = 3$). Species at the *right* sights of equations are stoichiometrically indistinguishable

relative standard deviation of A (typically 0.10 or 0.05) [26]. The model was considered as adequate if the following inequality held:

$$\chi^2_{\text{exp}} < \chi^2_f(5\ \%), \tag{4}$$

where $\chi^2_f(5\ \%)$ is the 5-% point of the Chi square distribution with $f = N - Z$ degrees of freedom.

The model admits the dependence of the affinity of sorption centers $\overline{Q_Z}$ to the probe on the degree of occupation of sorption centers. This allows to detect the cooperativity effects affecting the adsorption processes.

The software program CLINP 2.1 [27, 28] was used to calculate the stepwise equilibrium constants and equilibrium concentrations of species.

2.5 Voltammery and chronoamperometry experiments

The synthesized hybrid silica-organic material (SAM) and SAM with sorbed Cu (II) ions (Sample C from Table 1, SAM/Cu) were used to fabricate the working electrodes for electrochemical measurements. The electrodes (hereafter called SAM/C and SAM/Cu/C), disks of a 5 mm diameter and about 2 mm thickness, were prepared by mixing 23 mg of SAM or SAM/Cu with 23 mg of graphite and then pressing the mixtures under 3 tones. The resultant disks were glued to glass tubes with gel glue, maintained in a vertical positions facing downward and allowed to dry in air at a room temperature for 24 h. The electrical contact was made by a copper wire inserted inside the glass tube. In order to improve the connection between the wire and the disk surface, pure graphite powder was added to the glass tube.

The electrochemical experiments were performed at a room temperature with a PGSTAT20 potentiostat–galvanostat (Metrohm Autolab, the Netherlands), which includes the electrochemical cell with three electrodes. Saturated calomel electrode (SCE) and Pt wire were used as reference and auxiliary electrode, respectively. All potentials given in this paper are referred to the SCE, and all experiments were carried out at a room temperature in 1 mol l^{-1} KCl solution as supporting electrolyte.

3 Results and discussion

3.1 Characterization of the material

The prepared SAM material is disordered and consists of aggregated globular particles with the diameter of ~20–30 nm (Fig. 2). According to the results of the elemental analysis, specific concentrations are as follows: x(N) = 3.28 ± 0.05, x(C) = 10.73 ± 0.03 and x(H) = 29.4 ± 1.9 mmol g^{-1}. The specific concentration of amino groups is 3.28 ± 0.05 mmol g^{-1}, and the amount of silanol groups is comparable with that of amino groups. As the maximum attainable adsorption of H^+ ions is 2.34 ± 0.10 mmol g^{-1}, it may be concluded that more than 2/3 of immobilized amino groups are accessible for the H^+ probe. Specific surface area was 110 ± 2 m^2 g^{-1}, specific pore volume was 0.90 ± 0.01 cm^3 g^{-1}, and average pore size was 25 ± 3 nm. The structural information obtained from the ^{13}C and ^{29}Si CP/MAS NMR spectra is presented in Table 2.

According to the TGA analysis, the total weight loss 28 % was observed in the range of 30–700 °C. The

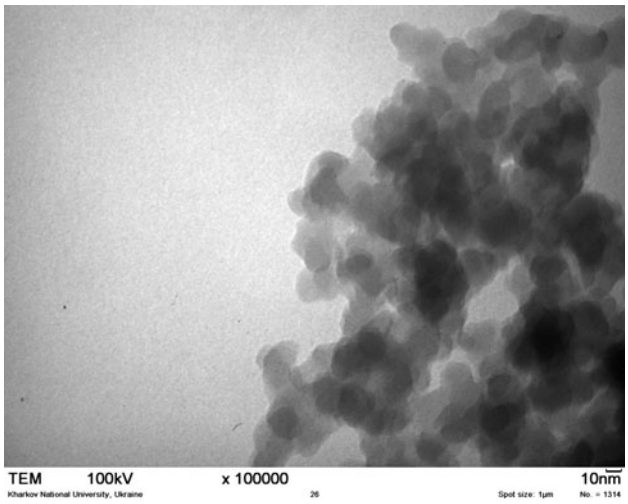

Fig. 2 TEM image of the material with immobilized amino groups

Table 2 Main NMR characteristics of the SAM material

^{29}Si NMR/ ppm	Assignment	^{13}C NMR/ ppm	Assignment
−56.7 (weak)	T_2 C–**Si**(OH)$(OSi)_2$	12.4	α H_2**C**–Si
−63.9	T_3 C–**Si**$(OSi)_3$	24.4	β CH_2–**C**H_2–CH_2
−86.6 (weak)	Q_2 **Si**$(OSi)_2(OH)_2$	45.3	γ H_2**C**–NH_2
−96.7	Q_3 $(OSi)_3$**Si**–OH		
−107.0	Q_4 **Si**$(OSi)_4$		

"Si" and "C" in bold help to perceive the attribution of signals in the spectra

following processes may be supposed: (a) removal of adsorbed water (70–135 °C, weight loss 9 %) [29]; (b) removal of chemically bonded water (200–300 °C) followed by the dehydroxylation (200–700 °C) [29] and (c) decomposition of *n*-propylamine groups (>280 °C) [30, 31].

Information about polarity and acidity of the near-surface layer of the SAM material was obtained from the results of probing the surface with the solvatochromic Reichardts' betaine dyes [21, 32]. Polarity was characterized by the Dimroth–Reichardt normalized polarity parameter, E_T^N [21]. The E_T^N values are estimated from the molar energies of the $\pi \rightarrow \pi^*$ electron transition accompanied by the intramolecular charge transfer in a molecule of a standard solvatochromic betaine dye ET(30). They are calculated from the position of maximum of the long-wave absorption band of the dye [32]. Water and tetramethylsilane are the standard solvents with E_T^N 1 and 0, respectively. The protonated form of ET(30) does not absorb light in the visible region and exhibits no solvatochromic effect. As its pK_a in aqueous solution is 8.64 [21], ET(30) is suitable for probing only neutral and basic media. Another solvatochromic betaine dye, ET(33), has $pK_a = 4.78$ [22] that makes it possible to probe not only basic but also neutral and weakly acidic media and to determine E_T^N values from the maxima of the ET(33) absorption bands.

Probing surfaces of silicas with grafted amino groups by ET(30) and ET(33) has revealed [33, 34] that regions with drastically different polarities and acidities coexist on surfaces. This was explained by the highly non-uniform (island-like) topography of the surfaces. One absorption band corresponds to the location of the probes in more acidic and more polar regions where unmodified silanol groups predominate, while another, more long-wave one appears when the probes are located in more basic and less polar regions formed by grafted amines.

Probing the SAM material by ET(30) has shown that at any accessible surface concentration of the dye the samples keep uncolored. This allows to conclude that (a) medium in the near-surface layer is rather acidic that falls in line with the presence of surface silanols detected by ^{29}Si NMR and elemental analysis, and (b) amino groups are distributed randomly and, in contrast to chemically modified silicas, do not form islands with high basicity. When probed the material with ET(33), only one wide absorbance band with maximum at ~460 nm was observed ($E_T^N = 0.64$) that points to the polarity of the near-surface layer close to those for water-organic mixtures and polar organic solvents rather than aqueous solutions.

Rather homogeneous distribution of immobilized amino groups concluded from the probing with solvatochromic dyes provides a possibility to estimate the average intermolecular distance between amino groups (l_i) on the base of the model proposed elsewhere [35]. The average surface density of amino groups

$$\delta = \frac{x\left((CH_2)_3NH_2\right) \times N_A}{S_{BET}} = 18 \text{ nm}^{-2}, \quad (5)$$

where N_A is the Avogadro's number, from which $l_{ij} = \delta^{-1/2} = 0.24$ nm.

The model of tridentate binding has described the equilibrium of H^+ ions adsorption adequately, while models of mono- and bidentate binding failed to approximate the experimental data in the limits of their errors (Table 3).

Based on the found values of equilibrium constants, it was concluded that negative cooperativity affects significantly the adsorption of H^+ ions (affinity of sorption centers to the probe is decreased with increasing the degree of protonization) [3].

The protonization constants of fixed amino groups are less by several orders than protonization constants of aliphatic amines in aqueous solutions. It means that basicity of amines is decreased when they fixed at the surface. As in the case of silicas with grafted amino groups, this is explained by interactions between surface amino groups and weakly acidic silanol groups. Thus, adsorption centers should be considered as assemblages of interacting immobilized amines and silanol groups [36].

The results of probing the material by H^+ ions were used to simulate the adsorption of Cu^{2+} ions. Model of tridentate binding describes well the competitive adsorption of H^+ and Cu^{2+} ions. The adequate description of experimental data was achieved in the model which took

Table 3 Characteristics of the H^+ adsorption by different versions of the model of polydentate binding

Z	$\log \beta_{Hi}^{(Z)}$			χ^2_{exp}	f	$\chi^2_f(5\ \%)$
	$i = 1$	$i = 2$	$i = 3$			
1	13 ± 100	–	–	8.7×10^5	13	22.3
2	7.7 ± 0.1	12.1 ± 0.1	–	66.4	12	21.0
3	8.0 ± 0.1	13.8 ± 0.1	17.5 ± 0.1	17.2	11	19.7

into account the formation of only one Cu (II) complex on the surface:

$$Cu^{2+} + \overline{Q_3} \overset{\beta_1^{(3)}}{=} \overline{CuQ_3}^{2+} \quad (6)$$

with $\log \beta_1^{(3)} = 5.5 \pm 0.1$, while $\beta_2^{(3)}$ and $\beta_1^{(3)}$ were negligibly small (the inclusion of complexes $\overline{Cu_2Q_3}^{4+}$ and $\overline{Cu_3Q_3}^{6+}$ into the model did not affect the quality of fitting the experimental data). So, strong negative cooperativity was concluded to affect the Cu^{2+} adsorption.

Only one wide band was observed in the absorption spectra of the material with adsorbed Cu^{2+} ions (Table 1). The values of the Kubelka–Munk function measured at the maximum of absorption depend linearly on specific concentrations of Cu^{2+} ions (correlation coefficient $r = 0.995$) that confirms the formation of complexes of only one type. The absorption maximum is due to the *d–d* transfer in the Cu (II) complex with the composition of coordination sphere $[Cu(\sim NH_2)(H_2O)_5]^{2+}$ (for the comparison: positions of the absorption maxima in the Cu (II) complexes with NH_3 and ethylendiamine (En) are as follows: $[Cu(NH_3)(H_2O)_5]^{2+}$ – 715–740 nm, $[Cu(NH_3)_2(H_2O)_4]^{2+}$ and $[CuEn(H_2O)_4]^{2+}$ – 660–690 nm, $[Cu(NH_3)_3(H_2O)_3]^{2+}$ – 630–645 nm [37]).

The determined equilibrium constants were used to calculate the yields of species in the adsorption systems dependently on pH of solutions, concentrations of reagents and ratios of the SAM material mass to the solution volume. The degrees of formation were calculated as

$$\alpha_i = \frac{\overline{[L_i]}}{\overline{[Q_3]} + \overline{[HQ_3^+]} + \overline{[H_2Q_3^{2+}]} + \overline{[H_3Q_3^{3+}]} + \overline{[CuQ_3^{2+}]}} \times 100, \%, \quad (7)$$

$$\gamma_{\overline{CuQ_3^{2+}}} = \frac{\overline{[CuQ_3^{2+}]} \cdot m_s/V}{[Cu^{2+}] + [CuOH^+] + \overline{[CuQ_3^{2+}]} \cdot m_s/V} \times 100, \%, \quad (8)$$

$$\gamma_{Cu^{2+}} = \frac{[Cu^{2+}] + [CuOH^+]}{[Cu^{2+}] + [CuOH^+] + \overline{[CuQ_3^{2+}]} \cdot m_s/V} \times 100, \%, \quad (9)$$

where square brackets denote equilibrium concentrations (specific for species on the material surface and molar for species in solution), upper lines relate to species on the surface, Q_3 represents free (not occupied with Cu^{2+} or H^+) binding centers, and L_i is Q_3, HQ_3^+, $H_2Q_3^{2+}$, $H_3Q_3^{3+}$ or CuQ_3^{2+}. Plots of α_i, $\gamma_{\overline{CuQ_3^{2+}}}$ and $\gamma_{Cu^{2+}}$ against pH of solutions presented in Fig. 3 were calculated for the following experimental conditions: $m_s = 0.100$ g, $V = 0.020$ l, total quantity of adsorption centers $n(Q) = 2.34 \times 10^{-4}$ mol, and total quantity of Cu (II) $n(Cu^{2+}) = n(Q) / 3 = 7.80 \times 10^{-5}$ mol.

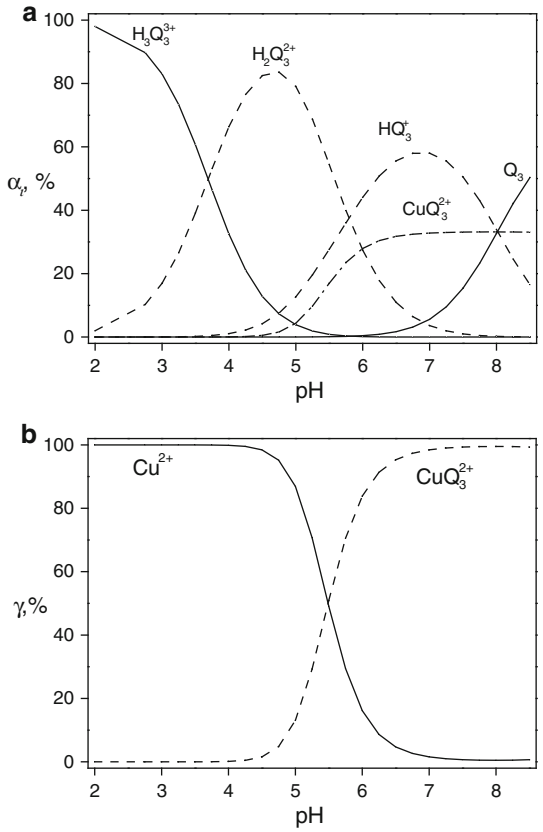

Fig. 3 Degrees of formation of species in the adsorption systems

According to the results of calculations, at pH < 4.5 only negligible quantities of Cu (II) are present on the material surface, at higher pH Cu (II) starts to adsorb, and at pH > 6.5 practically all Cu (II) is present in the system in the form of the surface complex. These conclusions are important for the choice of experimental conditions for the electrochemical measurements with the use of the SAM/Cu material.

3.2 Electrochemical determination of nitrite

3.2.1 Electrocatalytic oxidation of NO_2^- at the SAM/Cu/C electrode

The CVs obtained with the use of the SAM/C and SAM/Cu/C electrodes in 1 M KCl (pH 5.8) in the absence and presence of 0.4 mM NO_2^- were recorded in the potential range from −0.2 to 1.0 V (vs. SCE) (Fig. 4). The SAM/Cu/C electrode, as contrasted with the SAM/C one, demonstrates the electrochemical response (Fig. 4) that evidences the importance of the Cu (II) surface complex. Also, it becomes clear from this figure that this complex acts as a catalyst for the nitrite ions oxidation.

In the voltammogram obtained with the SAM/Cu/C electrode in the absence of NO_2^- ions the intense anodic

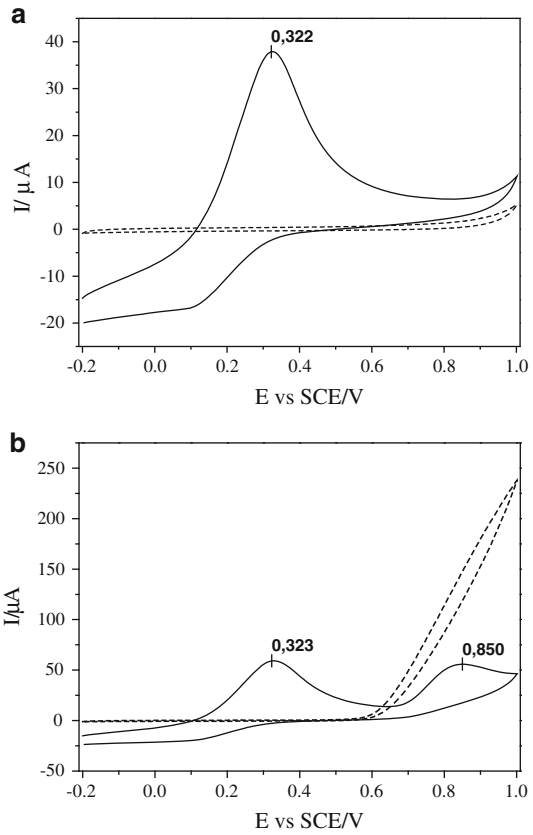

Fig. 4 CVs at SAM/C (*dash*) and SAM/Cu/C (*solid*) in 1 mol l^{-1} KCl (pH 5.8) with 0 (**a**) and 0.4 mmol l^{-1} NO_2^- (**b**). Scan rate: 20 mV s^{-1}

peak (I_{pa}) is observed at potential $E_{pa} = 0.322$ V versus SCE (Fig. 4a). This peak corresponds to the oxidation of Cu (I) species to Cu (II) ones [20, 38, 39]. The less distinctive cathodic peak (I_{pc}) is registered at $E_{pc} \approx 0.12$ V versus SCE. So, the formal potential $E^0 = (E_{pa} + E_{pc})/2 = (0.32 + 0.12)/2 = 0.22$ V. The comparison of Fig. 4 with the earlier published data [38, 39] witnesses that neither Cu (I) nor Cu (II) are reduced to Cu (0).

The Cu (I)/Cu (II) oxidation peak at the SAM/Cu/C electrode remains unchanged in the presence of nitrite ions. The electrode exhibits an excellent electrocatalytic activity toward the oxidation of NO_2^- to NO_3^- with the oxidation peak at $E_{pa} = 0.85$ V characteristic for the NO_2^- oxidation [15, 40]. This electrode was used as working in all electrochemical measurements.

3.2.2 *Effect of pH*

As stated above, retention or leaching of Cu (II) from the material depend on pH of solution. The exploitation of the SAM/Cu/C electrode in sufficiently acidic media is impossible because of the Cu (II) removal from the surface. On the other hand, in basic media $Cu(OH)_2$ precipitates and the material starts to dissolve that hinders the application of the electrode. Typical pH values of natural waters are between 5.0 and 8.5 (6.5–8.5 for river waters, 5.5–6.0 for swamp water, 4.6–6.1 for atmospheric precipitations, and 7.9–8.3 for seawater). Taking into account all these factors, the applicability of the SAM/Cu/C electrode was tested in the solutions with pH from 5.0 to 7.0.

The positions of the oxidation peak ($E_{pa} \approx 0.70$ V) and the anodic current ($I_{pa} \approx 20$ μA) at the DPV voltammograms (figure not shown) for the electrooxidation of NO_2^- (0.4 mM) in 1 M KCl remain practically invariant within the pH range from 5.0 to 7.0 that allow to use the SAM/Cu/C electrode at these values of pH. In the following experiments the supporting electrolyte solution with pH 5.8 was used. The invariability of the peak position suggests the oxidation of NO_2^- to be a proton independent catalytic step [40].

3.2.3 *Effect of scan rate*

The electrochemical reactivity of the SAM/Cu/C electrode was estimated by CVs in 1 M KCl containing 1.17 mM NO_2^- at the different scan rates. With the increase of the scan rate both anodic and cathodic peak currents for the Cu (I)/Cu (II) system increase, the cathodic peak potential is shifted towards negative values, and the anodic peak potential moves towards more positive values. For the couple NO_3^-/NO_2^-, when the scan rate increases, the anodic peak current and the positive shift in the peak position increase too (Fig. 5). The anodic peak current is linearly dependent on the square root of the scan rate (ν) in the range from 5×10^{-3} to 0.1 V s^{-1} ($r = 0.997$). This indicates that the rate-determining step of the electrocatalytic NO_2^- oxidation is the NO_2^- diffusion from solution [41].

Since the catalytic process behaves as a totally irreversible [42], the number of electrons involved in the

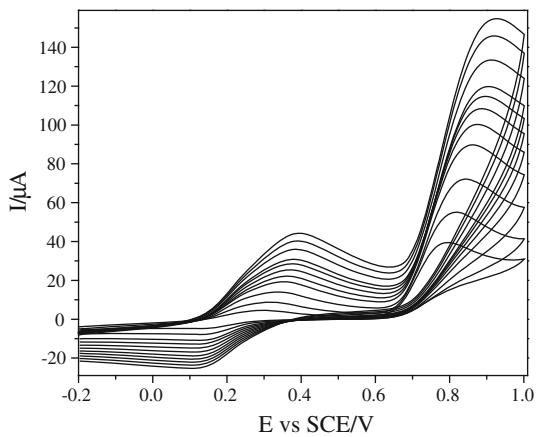

Fig. 5 CVs of the SAM/Cu/C electrode in 1 mol l^{-1} KCl (pH 5.8) containing 1.17 mmol l^{-1} NO_2^- at scan rates 5, 10, 20, 30, 40, 50, 60, 70, 80, 90 and 100 mV s^{-1}

overall reaction (n) can be obtained from the linear dependence of I_{pa} on $v^{1/2}$ [42, 43]:

$$I_{pa} = 2.99 \times 10^5 \cdot n \cdot [(1-\alpha)\cdot n_a]^{1/2} C(NO_2^-) A D_0^{1/2} v^{1/2} = G \cdot v^{1/2} \quad (10)$$

where the experimentally determined $G = 448 \times 10^{-6}$ A/(V $s^{-1})^{1/2}$, α is the electron transfer coefficient, n_a is the number of electrons involved in the rate-determining step, $C(NO_2^-) = 1.17 \times 10^{-6}$ mol cm^{-3}, A is the area of the electrode, cm^2, and the apparent diffusion coefficient of NO_2^- $D_o = 3.7 \times 10^{-5}$ cm^2 s^{-1} (the value of D_o was taken from [43]). The value of $(1-\alpha) \times n_a$ found from the relationship $(1-\alpha)n_a = \frac{46.9\times10^{-3}\ V}{|E_p - E_{p/2}|}$, where $E_{p/2}$ is the potential of the half peak, V [42, 43] is equal to 0.30. After substitution of all the numerical data in Eq. (10), the value of $n = 1.96$ was obtained. This means that NO_3^- ion is the main product of the oxidation of nitrite ions. The process of oxidation of nitrite ions at the SAM/Cu/C electrode can be represented by following equations:

$$CuQ_3^+ \rightarrow CuQ_3^{2+} + \bar{e}, \quad (11)$$

$$CuQ_3^{2+} + NO_2^- \rightarrow CuQ_3 \sim NO_2^+, \quad (12)$$

$$CuQ_3 \sim NO_2^+ + H_2O \rightarrow CuQ_3^+ + NO_3^- + 2H^+ + \bar{e}. \quad (13)$$

3.2.4 *Electrochemical determination of nitrite ions*

The cyclic voltammetry and the differential pulse voltammetry measurements show that the oxidation peak potentials of nitrite ions at the SAM/Cu/C electrode are linearly dependent on $C(NO_2^-)$ (r = 0.999, Figs. 6, 7). For DPV, the oxidation peak potential (+0.71 V) is shifted by 0.14 V to the negative direction as compared with the CV case. The advantages of DPV as compared with CV are the minimization of the capacitive charging current and the ohmic drop. In order to test the usefulness of the SAM/Cu/C electrode for the amperometric determination of nitrite, the chronoamperometric technique was used (Fig. 8). To obtain a highest current signal at the SAM/Cu/C electrode, the results of the DPV experiments were used. The maximum difference between currents for blank solution and solutions containing NO_2^- ions was observed at the applied potential 0.71 V (vs. SCE). So, the chronoamperometric measurements were performed at this value, and a linear dependence of the current on $C(NO_2^-)$ was observed.

The metrological characteristics of the determination procedures (Table 4) are comparable with the characteristics of the procedures reported earlier for other electrodes under similar experimental conditions (Table 5). They allow to determine nitrite ions in drinking water if their

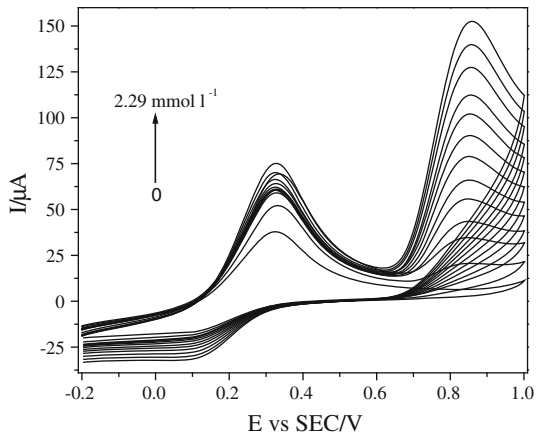

Fig. 6 CVs at the SAM/Cu/C electrode for different concentrations of nitrite ions. Potential scan rate: 20 mVs^{-1}; supporting electrolyte: 1.0 mol l^{-1} KCl; pH 5.8

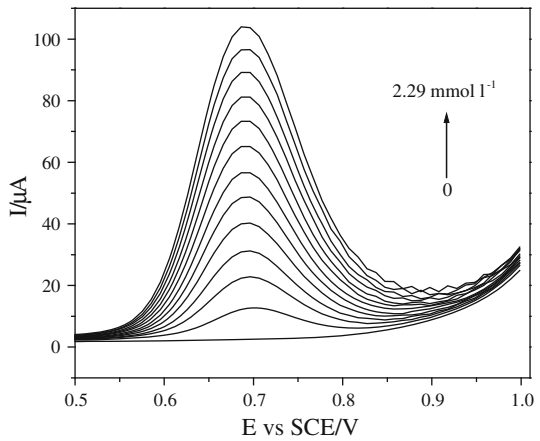

Fig. 7 DPVs at the SAM/Cu/C electrode for different concentrations of nitrite ions. Supporting electrolyte: 1.0 mol l^{-1} KCl; pH 5.8

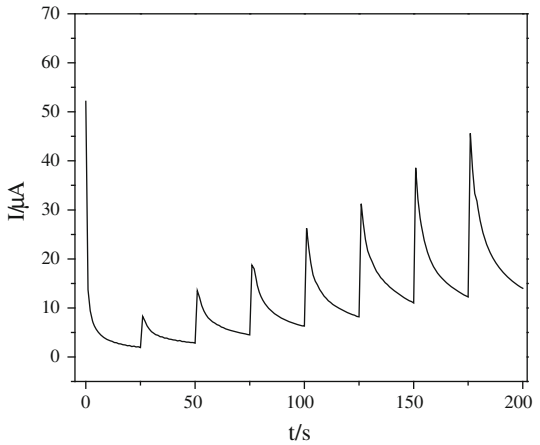

Fig. 8 Chronoamperograms at the SAM/Cu/C electrode at a fixed potential 0.71 V. Supporting electrolyte is 1 mol l^{-1} KCl; pH 5.8

Table 4 Metrological characteristics of the determination procedures

Procedure	Analytical range/μmol l^{-1}	LOD/ μmol l^{-1} [a]	LOQ/ μmol l^{-1}[a]	Sensitivity (k)/μA l $mmol^{-1}$	Repeatability (relative standard deviation, %)[b]	Reproducibility (relative standard deviation, %)[b]
CV	4–2,300	1.32 ± 0.02	4.00 ± 0.03	62.3 ± 0.7	0.6	4.8
DPV	14–2,300	4.62 ± 0.04	14.2 ± 0.5	43.6 ± 0.3	0.9	5.4
ChA	9–700	3.08 ± 0.05	9.33 ± 0.04	62.5 ± 1.4	1.3	5.8

[a] LOD (limit of detection) and LOQ (limit of quantification) were estimated from equations $I_{LOD} = I_0 + 3 \cdot \sigma$ and $I_{LOQ} = I_0 + 10 \cdot \sigma$, where I_0 is the analytical signal of the blank, and σ is its standard deviation [44]

[b] Repeatability was estimated from five experiments performed on the same day, in the same electrochemical cell with the same samples containing 1.7 mmol l^{-1} NO_2^- (for CV and DPV) and 0.4 mmol l^{-1} NO_2^- (for ChA), and reproducibility was determined in a series of experiments with five different electrodes prepared in the same manner

Table 5 Metrological characteristics of the procedures for the determination of nitrite ions

Electrode	Procedure	Analytical range/μmol l^{-1}	LOD/μmol l^{-1}	Sensitivity/μA l $mmol^{-1}$	pH	References
NPGL/GCE[b]	ChA	1–1,000	–	130	4.5	[15]
Au/PAni/GCE[a]	DPV	0.4–5,000	0.2	7.2	3.0	[45]
SiO_2/Cyt c/SiO_2/BDDE[c]	ChA	1–1,000	0.5	13.5	6.86	[46]
AgNP/GC[d]	ChA	10–1,000	1.2	100	6.0	[47]
	CV	50–600	–	35	6.0	

[a] Gold particles/polyaniline modified glassy carbon electrode

[b] Nanoporous gold leaf modified glassy carbon electrode

[c] Silica–gel/cytochrome boron-doped diamond electrode

[d] Silver nanoplates modified glassy carbon electrode

concentration corresponds to the maximum admissible concentrations (11–65 μmol l^{-1}) [10, 11] or exceeds them.

The stability of the SAM/Cu/C electrode was checked by recording successive cyclic voltammograms. In the presence of nitrite (1.7 mM), only minor changes were observed in the voltammetric profiles after 100 cycles. The electrode can be kept at a room temperature for at least 3 month without loss of its characteristics. Before every measurement clean and air-dried surface of the electrode should be polished carefully. Invariability of the electrode may be explained by the sufficient stability of the material deduced from the TGA results and by the strong bonding of Cu (II) ions with surface amino groups.

The DPV procedure has the worst metrological characteristics among all discussed here, and its applicability for the analysis of real objects will testify to the practical utility of the SAM/Cu/C electrode. So, DPV was used to analyze a natural water sample for the NO_2^- content. Three river water samples (pH 6) from the Barao Geraldo district (Campinas) were collected. After filtration, 3 ml of Britton–Robinson buffer solution with pH 5.8 were added to 50 ml of the sample solution, and the precise weights of KCl were dissolved to make the supporting electrolyte concentration 1 mol l^{-1}. Then the amount of nitrite in the samples was determined by the standard addition method (Table 6).

Table 6 Determination of nitrite ions in the river water by the standard addition method

NO_2^- added/ μmol l^{-1}	NO_2^- expected/ μmol l^{-1}	NO_2^- found/ μmol l^{-1}	Recovery/ %
0	–	39.2 ± 0.9	–
21.8	60	60.8 ± 0.7	101 ± 1
80.5	119.7	118.3 ± 0.7	99 ± 1

4 Conclusions

Hybrid silica-organic material with immobilized amino groups was prepared by sol–gel method from APTES and TEOS with almost complete transformation of ethoxy groups. The material consists of globules ~20–30 nm in diameter. The material demonstrates high thermal stability. The elemental analysis shows comparable concentrations of silanol groups and immobilized amino groups. Probing of the material surface with the solvatochromatic Reichardts' betaine dyes reveals relatively homogeneous (non-island) topography of the surface (that distinguishes this material from silicas with grafted amino groups) and the polarity of the near-surface layer close to that for water-organic mixtures and polar organic solvents. The decrease of the basicity of amino groups as the result of the

immobilization, concluded from probing the material surface with solvatochromatic betaine dyes and H^+ ions, is due to the interaction of surface silanol and amino groups. Protolytic properties of immobilized amino groups and their interaction with Cu (II) ions were described by the model of polydentate binding, and the influence of strong negative cooperativity effects on the adsorption equilibria was detected. The material with adsorbed Cu (II) ions was used to develop the working electrode suitable for the voltammetric and chronoamperometric determination of nitrite ions. Information about protolytic and complexing properties of fixed amines has allowed to adjust the optimal conditions for the analytical application of the electrode. The electrode is easily fabricated, may be kept for a long time without change of its characteristics, and exhibits high electrocatalytic activity to the nitrite oxidation. The procedures for the determination of nitrite ions in aqueous media by CV, DPV and ChA were developed with the use of the electrode. They have a broad analytical range, good repeatability and reproducibility.

Acknowledgments This work was financially supported by Ministry of Education and Science of Ukraine through Project No 0109U001310. O.T. is indebted to this Ministry for the financial support of his in-depth training in the State University of Campinas. Authors are deeply grateful to Professor Alexander Korobov for manuscript revision and to Mr. Sergey Shekhovtsov for synthesis and purification of ET(33).

References

1. Doyle AM, Hodnett BK (2006) J Non-Crystal Solids 352: 2193–2197
2. Franc J, Blanc D, Zerroukhi A, Chalamet Y, Last A, Destouches N (2006) Mater Sci Eng, B 129:180–185
3. Lucho AMS, Panteleimonov A, Kholin Y, Gushikem Y (2007) J Colloid Interface Sci 310:47–56
4. Dana E, Sayari A (2011) Chem Eng J 166:445–453
5. Aguado J, Arsuaga JM, Arencibia A, Lindo M, Gascon V (2009) J Hazard Mater 163:213–221
6. Echeverria JC, Vicente P, Estella J, Garrido JJ (2012) Talanta 99:433–440
7. Arguello J, Magosso HA, Landers R, Gushikem Y (2008) J Electroanal Chem 617:45–52
8. Silveira G, Morais A, Villis PCM, Maroneze CM, Gushikem Y, Lucho AMS, Pissetti FL (2012) J Colloid Interface Sci 369:302–308
9. Arguello J, Magosso HA, Landers R, Pimentel VL, Gushikem Y (2010) Electrochim Acta 56:340–345
10. Sands P, Galizzi P (2006) Documents in European Community Environmental Law, 2nd edn. Cambridge University Press, Cambridge
11. World Health Organization (2008) Guidelines for drinking-water quality, 3rd edn. WHO Press, Geneva
12. Senra-Ferreiro S, Pena-Pereira F, Lavilla I, Bendicho C (2010) Anal Chim Acta 668:195–200
13. Hea L, Zhang K, Wanga C, Luo X, Zhang S (2011) J Chromatogr A 1218:3595–3600
14. Nilsson KF, Lundgren M, Agvald P, Adding LC, Linnarsson D, Gustafsson LE (2011) Biochem Pharmacol 82:248–259
15. Ge X, Wang L, Liu Z, Ding Y (2011) Electroanal 23:381–386
16. Santos WJR, Lima PR, Tanaka AA, Tanaka SMCN, Kubota LT (2009) Food Chem 113:1206–1211
17. Kerkeni S, Lamy-Pitara E, Barbier J (2002) Catal Today 75:35–42
18. Li J, Lin X (2007) Microchem J 87:41–46
19. Rocha JRC, Angnes L, Bertotti M, Araki K, Toma HE (2002) Anal Chim Acta 452:23–28
20. Borgo CA, Ferrari RT, Colpini LMS, Costa CMM, Baesso ML, Bento AC (1999) Anal Chim Acta 385:103–109
21. Reichardt C, Welton T (2010) Solvents and solvent effects in organic chemistry, 4th edn. WILEY-VCH, Weinheim
22. Kessler MA, Wolfbeis OS (1989) Chem Phys Lipids 50:51–56
23. Britton HTS, Robinson RA (1931) J Chem Soc 1:458–473
24. Morosanova EI, Velukorodniy AA, Kyzmin NM, Zolotov YuA (1999) Patent 2139244 Russ Federation, IPC C01B33/12, G01N31/00
25. Brunauer S, Emmett PH, Teller E (1938) J Am Chem Soc 60:309–319
26. Bugaevsky AA, Kholin YV (1991) Anal Chim Acta 249:353–356
27. Merny SA, Konyaev DS, Kholin YV (1998) Kharkov Univ Bulletin 420:112–120
28. http://www-chemo.univer.kharkov.ua/kholin/clinp.html
29. Brambilla R, Poisson J, Radtke C, Miranda MSL, Cardoso MB, Butler IS, Santos JHZ (2011) J Sol-Gel Sci Technol 59:135–144
30. Luan Z, Fournier JA, Wooten JB, Miser DE (2005) Microporous Mesoporous Mater 83:150–158
31. Zub YL, Stolyarchuk NV, Barczak M, Dabrowski A (2010) Appl Surf Sci 256:5361–5364
32. Reichardt C (2007) Org Process Res Dev 11:105–113
33. Duncan JM, Tavener SJ, Gray GW, Heath PA, Rafelt JS, Saulzet SI, Hardy JJE, Clark JH, Sutra P, Brunel D, Renzo F, Fajula F (1999) New J Chem 23:725–731
34. Khristenko IV, Kholin YV, Mchedlov-Petrossyan NO, Reichardt C, Zaitsev VN (2006) Colloid J 68:511–517
35. Denofre S, Gushikem Y, Castro SC, Kawano Y (1993) J Chem Soc, Faraday Trans 89:1057–1061
36. Kholin Y, Zaitsev V (2008) Pure Appl Chem 80:1561–1592
37. Volchenskova II (1973) Theor Exp Chem 9:495–501
38. Shaikh AA, Firdaws J, Badrunnessa SS, Rahman MS, Bakshi PK (2011) Int J Electrochem Sci 6:2333–2343
39. do Carmo DR, Paim LL, Silvestrini DR, de Sa AC, de Oliveira Bicalhol U, Stradiotto NR (2011) Int J Electrochem Sci 6:1175–1188
40. Sljukic B, Banks CE, Crossley A, Compton RG (2007) Electroanal 19:79–84
41. Maroneze CM, Arenas LT, Luz RCS, Benvenutti EV, Landers R, Gushikem Y (2008) Electrochim Acta 53:4167–4175
42. Bard AJ, Faulkner LR (2001) Electrochemical methods, fundamentals and applications, 2nd edn. Wiley, New York
43. Sousa AL, Santos WJR, Luz RCS, Damos FS, Kubota LT, Tanaka AA, Tanaka SMCN (2008) Talanta 75:333–338
44. Currie LA (1995) Pure Appl Chem 67:1699–1723
45. Hao Y, Liu Y, Hao B (2011) In: Cao Z, Cao X, Sun L, He Y (eds) Advanced Materials Research, vol 239–242. Trans Tech Publications, Switzerland, pp 2466–2469
46. Geng R, Zhao G, Liu M, Li M (2008) Biomater 29:2794–2801
47. Wang Z, Liao F, Guo T, Yang S, Zeng C (2012) J Electroanal Chem 664:135–138